Chemistry
A European
Journal

Chemistry Europe
European Chemical Societies Publishing

Accepted Article

Title: The effects of ring strain on cyclic tetraaryl[5]cumulenes

Authors: Bozheng Sun, Meagan S. Oakley, Kota Yoshida, Yanwen Yang, Matteo Tommasini, Chiara Zanchi, Andrea Lucotti, Michael J. Ferguson, Frank Hampel, Mariusz Klobukowski, and Rik R. Tykwinski

To be cited as: *Chem. Eur. J.* **2022**, e202200616

Link to VoR: https://doi.org/10.1002/chem.202200616

WILEY-VCH

The effects of ring strain on cyclic tetraaryl[5]cumulenes

Bozheng Sun,[a] Dr. Meagan S. Oakley,[a] Dr. Kota Yoshida,[b] Yanwen Yang,[a] Prof. Matteo Tommasini,[c] Dr. Chiara Zanchi,[c] Dr. Andrea Lucotti,[c] Dr. Michael J. Ferguson,[a] Dr. Frank Hampel,[d] Prof. Mariusz Klobukowski,[a] and Prof. Rik R. Tykwinski[a]*

[a] Department of Chemistry, University of Alberta, Edmonton AB T6G 2G2 (Canada)
*rik.tykwinski@ualberta.ca, orcid.org/0000-0002-7645-4784

[b] Department of Chemistry, Graduate School of Science, Kyoto University, Kyoto 606-8502 (Japan)

[c] Dipartimento di Chimica, Materiali e Ingegneria Chimica "Giulio Natta", Politecnico di Milano, Piazza Leonardo da Vinci 32, 20133, Milano (Italy)

[d] Department of Chemistry and Pharmacy & Interdisciplinary Center for Molecular Materials (ICMM), University of Erlangen-Nuremberg, Nikolaus-Fiebiger Str. 10, 91058 Erlangen (Germany)

Bozheng Sun**:** orcid.org/0000-0003-3644-6103

Meagan S. Oakley: orcid.org/0000-0001-5072-7572

Yanwen Yang: 0000-0002-9911-0300

Matteo Tommasini: orcid.org/0000-0002-7917-426X

Chiara Zanchi: orcid.org/0000-0003-2656-7040

Andrea Lucotti: orcid.org/0000-0003-2148-1408

Michael J. Ferguson: orcid.org/0000-0002-5221-4401

Frank Hampel: orcid.org/0000-0001-9768-782X

Mariusz Klobukowski: orcid.org/0000-0001-9232-9900

10.1002/chem.202200616

Abstract: Cyclic tetraaryl[5]cumulenes (**1a–f**) have been synthesized and studied as a function of increasing ring strain. The magnitude of ring strain is approximated by the extent of bending of the cumulenic core as assessed by a combination of X-ray crystallographic analysis and DFT calculations. Trends are observed in ^{13}C NMR, UV-vis, and Raman spectra associated with ring strain, but the effects are small. In particular, the experimental HOMO–LUMO gap is not appreciably affected by bending of the [5]cumulene framework from ca. 174° (λ_{max} = 504 nm) in **1a** to ca. 178° (λ_{max} = 494 nm) in **1f**.

10.1002/chem.202200616

Introduction. Macrocycles hold unique allure to organic chemists.[1,2] They often present beautiful synthetic targets, but syntheses can also be challenging to accomplish due the increased entropic penalty from cyclization. Conjugated macrocycles are a particularly attractive subclass of macrocycles that offer a rigid/semi-rigid substrate to study aromaticity,[3–5] host-guest complexation,[6] and new materials,[7,8] just to name a few.[9,10] Composed of sp^2- and sp-hybridized carbon, the synthesis of conjugated macrocycles often faces an additional challenge in comparison to their linear or planar acyclic analogues, as ring formation leads to deformation of the ideal bond angles of 120 and 180°, respectively, resulting in ring strain.[11,12] Furthermore, increased macrocyclic strain often creates challenging syntheses as less "stable" products become more reactive and difficult to isolate. On the other hand, ring strain can also be advantageous and harnessed for selective reactivity patterns.[13]

Strained, carbon-based macrocycles have long been studied, and most recently the studies of cycloparaphenylenes (CPPs) and cycloparaphenyleneacetylenes are noteworthy milestones.[14–16] The influence of strain on the properties is well documented in these and other systems, as changes in orbital overlap as a function of strain often produces consistent trends in e.g., electronic properties that depend on HOMO and LUMO energy levels.[15,17] The cyclo[*n*]carbons are specific class of macrocycles,[18,19] and composed of only carbon they are considered molecular carbon allotropes, the cyclic analogs of the linear carbon allotrope carbyne (Figure 1a).[20,21] The synthesis of any member of this class of molecules in solution has so far been unsuccessful, although examples have been studied in the gas phase[18,19,22] and their formation proposed in a frozen matrix.[23] A remarkable surface synthesis of *cyclo*-C_{18}[24,25] has recently been reported that has both renewed the excitement in this class of molecules and provided the first evidence that the structure is like polyynic rather than cumulenic (Figure 1b).

The link between electronic properties and the configuration of π-orbitals is a long-standing question. Macrocyclic strain influences the energy levels of both the HOMO and the LUMO as bond angles about the sp^2- and sp-hybridized carbons deviate from the ideal values due to the ring strain.[26] This relationship is obvious, for example, as one transitions from planar materials such as oligophenylenes and graphene to cyclic analogs such CPPs and carbon nanotubes, respectively.

Macrocyclic strain is also a key consideration in the formation of the cyclo[*n*]carbons. In the absence of solution-state synthesis of cyclo[*n*]carbons, partially conjugated model compounds can serve as a platform to analyze stability and properties as strain is increased. Strained tetraynes have been explored (Figure 1c), indicating that a stability limit for solution-state characterization is reached at approximately the 1,2,3,4-heptadecatetrayne.[27] The study of strained cyclic [*n*]cumulenes, however, is limited to reports of cyclic [3]cumulenes[28] that confirmed that 1,2,3-cycloctatriene can be formed and trapped[29] while 1,2,3-cyclononatriene is the smallest isolable derivative (Figure 1c).[30] Thus, the stability and the effects of strain on electronic and structural properties of cyclic cumulenes remains limited.

We report herein the formation of a series of cyclic [5]cumulenes, molecules **1a–f** (Figure 1c).[31] Each compound features a tetraaryl[5]cumulene moiety tethered by an alkyl chain that can be systematically shortened to increase strain. [5]Cumulenes were chosen for this study as it is well established that longer odd [*n*]cumulenes (*n* is an odd number) with $n \geq 7$ typically lack kinetic stability under ambient conditions even for unstrained systems.[32,33] The effect of the ring strain on [5]cumulenes **1a–f** is then evaluated through computational, spectroscopic, and crystallographic analyses.

10.1002/chem.202200616

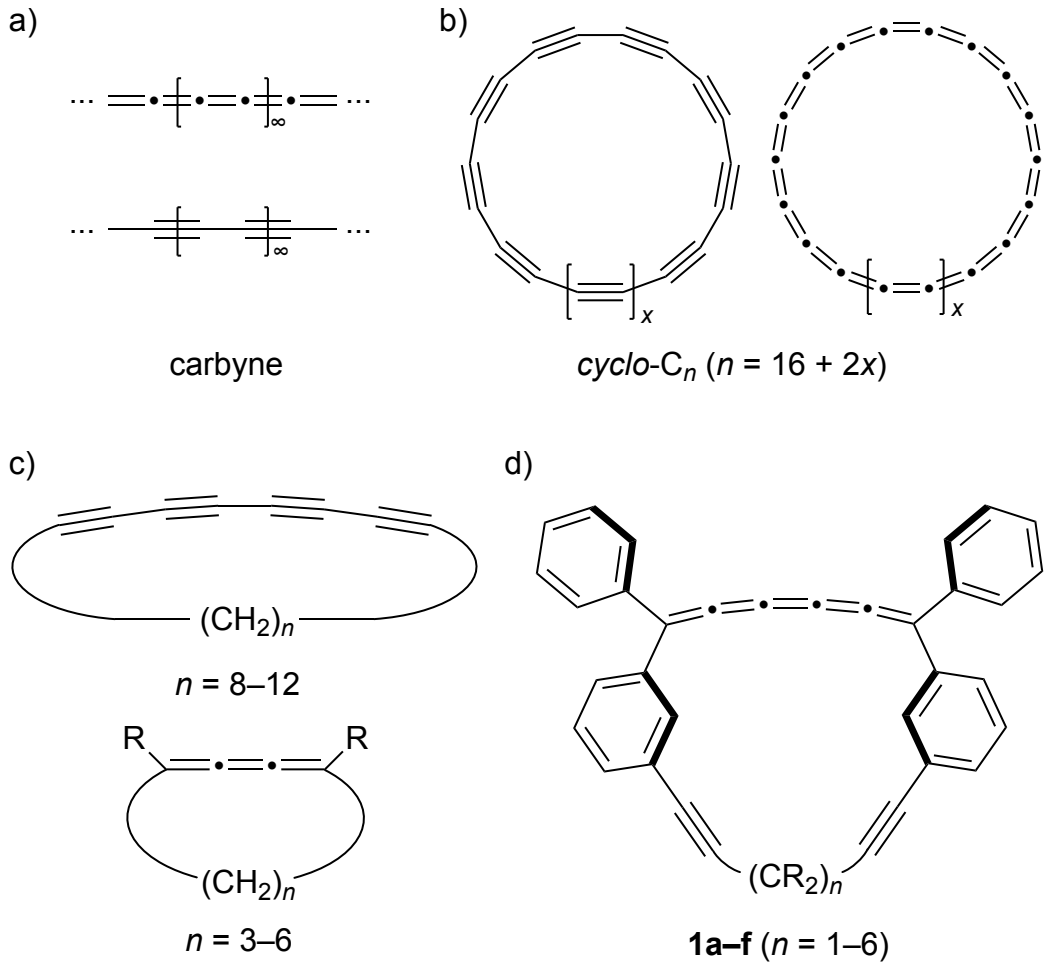

Figure 1. a) Schematic representation of the cumulenic (top) and polyynic (bottom) form of the sp-hybridized carbon allotrope carbyne; b) Polyynic and cumulenic isomers of the molecular carbon allotropes *cyclo*-C$_n$; c) Tetraynes (reference **Error! Bookmark not defined.**) and [3]cumulenes (reference **Error! Bookmark not defined.**) used to explore macrocyclic strain (left); d) Cyclic [5]cumulenes studied in this work (right).

10.1002/chem.202200616

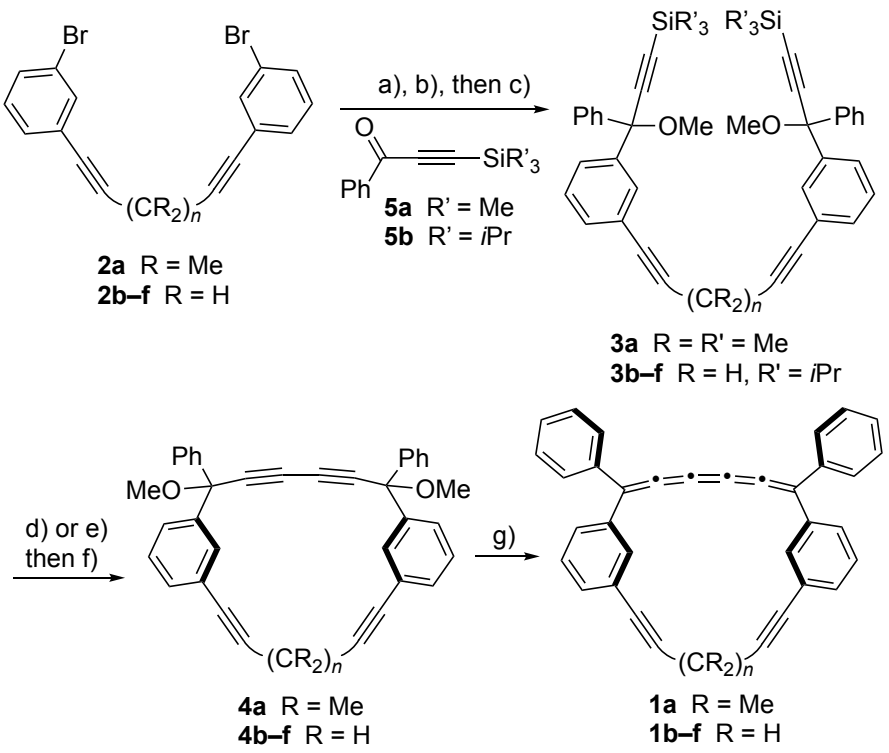

Scheme 1. Synthesis of cyclic [5]cumulenes **1a–f**. a) *n*BuLi, THF, –78 °C; b) **5a** or **5b**; c) MeI, –78 °C to rt; d) K_2CO_3, MeOH, rt; e) TBAF, THF, H_2O, rt; f) CuCl, $Cu(OAc)_2$, pyridine, rt. g) $SnCl_2$, HCl in Et_2O, THF, rt; TBAF = tetra-*n*-butylammonium fluoride.

Table 1. Isolated yields for compound **1**, **3**, and **4**.

compound	*n*	R	R'	**3** yield (%)	**4** yield (%)	**1** yield (%)
a	1	Me	*i*Pr	55[a]	40[c,e]	43
b	2	H	Me	37[b]	52[d,e]	66
c	3	H	Me	53[b]	37[d,e]	32
d	4	H	Me	51[b]	47[d,e]	55
e	5	H	Me	41[b]	23[d,e]	40
f	6	H	Me	44[b]	62[d,e]	59

[a] Using **5a**. [b] Using **5b**. [c] Desilylation using K_2CO_3, MeOH. [d] Desilylation using TBAF. [e] Yield over two steps from **3**.

The synthetic design of **1a–f** relied on a common approach starting with **2a-f** which define the length of the alkyl chain serving as the tether. Aryl bromides **2a-f** are readily elaborated to **3a–f** to complete the carbon skeleton, followed by cyclization to **4a–f**, and reductive elimination (Scheme 1). Tethers **2a–f** with a varied number of methylene units were formed from the corresponding diyne and 3-bromoiodobenzene using a Sonogashira reaction (see SI for details). The structure of tether **2a** incorporated the isopropylidene group in order to circumvent known rearrangements with the unsubstituted 1,4-pentadiyne substructure under basic conditions.[34] The treatment of **2a–f** with two equivalents of *n*BuLi was followed by the addition of a slight excess of either ynone **5a** or **5b**. Quenching of the reaction with MeI effected *O*-methylation of the alcoholate intermediate and afforded **3a–f**. The terminal alkynes were liberated via removal of the silyl protecting groups via reaction with either K_2CO_3/methanol or TBAF, and a subsequent intramolecular Eglinton-Galbraith homocoupling gave cyclic alkynes **4a–f**. The cyclization was conducted under high dilution (ca. 0.4 mM) to reduce intermolecular homocoupling that would lead to side products through either dimerization or polymerization. Finally, reductive elimination[35] in the presence of $SnCl_2$ and HCl afforded the desired cyclic [5]cumulenes **1a–f**.

The transformation from **4a–f** to **1a–f** is ready established by spectroscopic analyses. ^{1}H NMR spectroscopy confirms successful removal of methoxy groups through loss of the Me resonances. The ^{13}C NMR spectra of **1a–f** show loss of carbon resonances of the butadiyne moiety, as well as the appearance of resonances consistent with the cumulenic framework (vide infra). Finally, MALDI HRMS clearly shows signals consistent with [M^+] for each cumulenic product, and the structures of macrocycles **1a–e** have ultimately been established by XRD analyses.

All of the isolated cyclic [5]cumulenes **1a–f** are sufficiently stable for purification and routine characterization, although compounds **1a** and **1b** are less stable than **1c–f** under ambient

10.1002/chem.202200616

conditions. When **1a** is stored in chloroform solution at room temperature for several days, a number of decomposition products are observed by TLC, and the cross-conjugated,[36] four-fold symmetric [4]radialene **6** could be chromatographically isolated (Figure 2). Spectroscopic characterization strongly suggests that only one isomer is formed, although it could not be established if it is the *syn*- or *anti*-isomer. It has been reported that tetra-*t*-butyl-,[37] tetraphenyl-,[38] and tetra(3,5-*t*-butylphenyl)-[5]cumulenes[39] can dimerize into a radialene structure when heated. The dimerization of [5]cumulenes under Ni-catalysis has also been reported by Iyoda and coworkers.[40] In the present case, the conversion of **1a** to radialene **6** at room temperature in the absence of catalyst suggests that reactivity is potentially augmented by ring stain with concurrent rehybridization at C2–C5 due to poor p-orbital overlap.[17,28] It should be noted, however, that calculations have shown that even moderate bending of the cumulene moiety in cyclic 1,2,3-butatrienes (ca. 15°) results in only a mild increase in strain energy, concurrent with enhanced reactivity.[41]

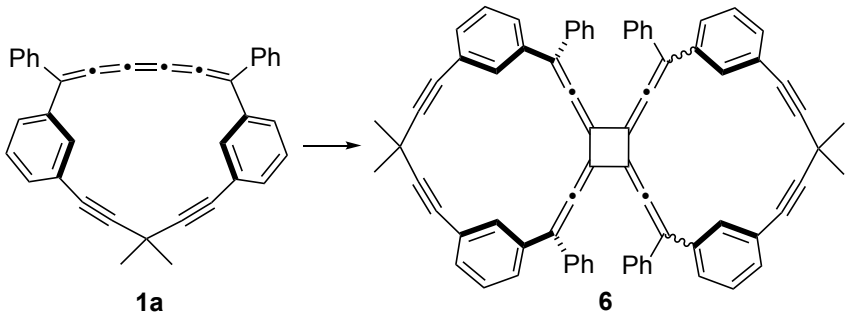

Figure 2. Formation of dimer **6**.

Structural analysis. Single crystals of **1a–e** suitable for X-ray crystallographic analysis (XRD) were grown at rt, by a slow diffusion of a dichloromethane solution of the corresponding macrocycle layered with methanol (Figure 3).[42] The cumulenic bond angles of compounds **1a–e** from XRD confirm increased bending as the length of the alkyl chain is decreased from **1e** to **1a**

(Table 2). Notably, none of the solid-state structures show planar or rotational symmetry, and analogous angles (e.g., C1–C2–C3 and C4–C5–C6) often feature different degrees of bending. As a means of comparison, the average bond angles (BA_{avg}) have been calculated from the bond angles C1–C2–C3, C2–C3–C4, C3–C4–C5, and C4–C5–C6 and decrease from BA_{avg} = 178.1° in **1e** to BA_{avg} = 173.9° in **1a**. The average bond angle of **1a** is smaller than those of other reported crystal structures of cumulenes, except for the acyclic [3]cumulene 1,1,4,4-tetrakis(3,5-di-*tert*-butylphenyl)buta-1,2,3-triene,[43] which shows bond angles of 168.31° and 169.47° (BA_{avg} = 168.9°) as a result of dispersive interactions between aryl and *tert*-butyl groups across the cumulenic core. An odd-even disparity is evident, as BA_{avg} values for odd alkyl chains (with an odd number of methylene groups, n = 3 and 5) resemble those of the even chains featuring one carbon less.

There is an obvious challenge with overreliance on crystallographic data, namely, XRD provides information for only one of potentially many structures as a results of packing forces in the solid state. Thus, the structures of **1a–f** have been probed by density functional theory calculations with the PBE0 functional[44] and cc-pVTZ[45] basis set, and geometries were optimized in both the gas phase and with an implicit dichloromethane solvent (Table 2). An important comparison of XRD and computed structures is the relative planarity of the pendent aryl groups to the cumulenic framework, which extends conjugation and has been shown to affect both bonding and electronic structure.[33] In comparison to values derived from XRD, calculated torsion angles between the cumulene and aryl groups follow similar trends (Table S4), supporting the use of solid-state structures for comparisons (a similar analysis is consistent with Raman data, vide infra). Furthermore, comparison of BA_{avg} values for **1a–e** shows that values from calculations are slightly greater than those determined by XRD, although the difference is less than 0.9° in all cases. DFT

calculations have also been used to estimate strain energies for **1a–f** through a homodesmotic reaction scheme (see SI for details).[41,46] While calculations confirm that strain decreases as ring size increases, energies vary by only ca. 2 kcal/mol throughout the series.

Analysis of bond lengths shows little variance of analogous lengths upon ring contraction from **1e** to **1a** (Table 2) for either XRD or computational analyses. Likewise, bond length alternation (BLA) values showed no discernable trend as a function of increasing strain (BLA calculated as the bond-length difference between C3–C4 and the average of C2–C3 and C4–C5). Calculated BLA values are, however, consistently less than those determined experimentally.

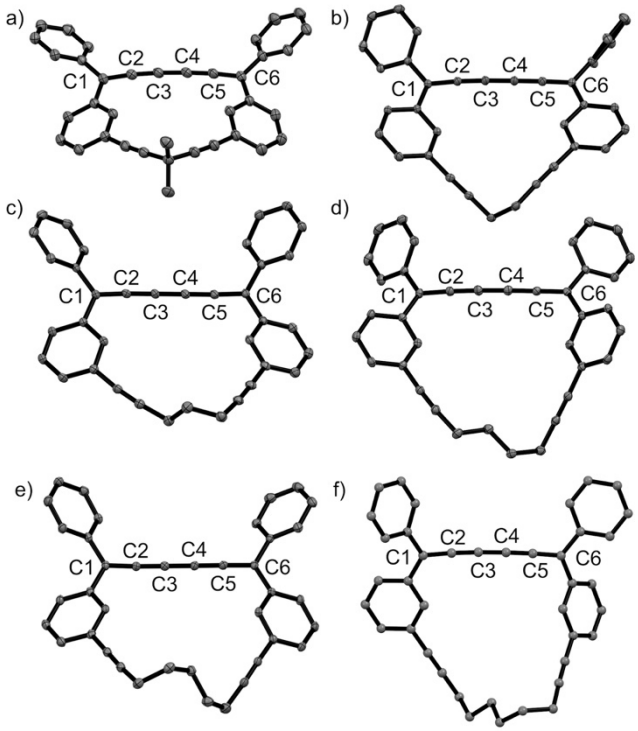

Figure 3. a–e) ORTEP structures of cyclic [5]cumulenes **1a–e**, respectively, as determined by X-ray crystallography (H atoms removed for clarity; ORTEPs shown at 30% probability level); f) calculated structure of **1f** (optimized in the gas phase at the PBE0/cc-pVTZ level of theory).

10.1002/chem.202200616

Table 2. Selected structural data, bond angles [°], and bond lengths (Å) for compounds **1a–f** as determined by X-ray crystallography and DFT calculations.[a]

cmpd	method	C1–C2–C3	C2–C3–C4	C3–C4–C5	C4–C5–C6	BA_{avg}[b]	C1–C2	C2–C3	C3–C4	C4–C5	C5–C6	BLA[c]
1a	XRD[d]	172.3(3)	174.4(3)	175.1(3)	173.7(3)	173.9	1.346(4)	1.250(4)	1.318(4)	1.252(4)	1.346(4)	0.0670
1a	GP[e,f]	173.66	174.55	174.55	173.66	174.11	1.3362	1.2534	1.2963	1.2534	1.3362	0.0429
1a	DCM[e,g]	173.78	174.49	174.49	173.78	174.14	1.3369	1.2538	1.2969	1.2538	1.3369	0.0432
1b	XRD[d]	172.49(12)	175.10(12)	175.27(11)	175.66(10)	174.63	1.3405(14)	1.2528(15)	1.3042(14)	1.2489(15)	1.3444(14)	0.05335
1b	GP[e,f]	175.17	175.33	175.34	175.18	175.26	1.3352	1.2528	1.2958	1.2528	1.3352	0.0430
1b	DCM[e,g]	175.31	175.18	175.17	175.31	175.24	1.3359	1.2531	1.2965	1.2531	1.3359	0.0433
1c	XRD[d]	175.4(3)	176.4(3)	176.5(3)	176.9(3)	176.3	1.342(3)	1.253(4)	1.306(4)	1.252(4)	1.345(3)	0.0535
1c	GP[e,f]	174.68	176.95	177.32	178.60	175.89	1.3363	1.2536	1.2962	1.2539	1.3352	0.0426
1c	DCM[e,g]	175.01	176.92	177.37	178.48	176.95	1.3369	1.2540	1.2968	1.2543	1.3359	0.0428
1d	XRD[d]	179.8(4)	177.8(4)	178.1(5)	177.2(5)	178.2	1.337(5)	1.258(5)	1.313(5)	1.249(5)	1.346(5)	0.05[illegible]
1d	GP[e,f]	179.68	178.99	178.71	177.50	178.72	1.3348	1.2539	1.2959	1.2536	1.3356	0.042[illegible]
1d	DCM[e,g]	177.77	178.77	179.14	179.72	178.85	1.3363	1.2541	1.2966	1.2544	1.3356	0.425
1e	XRD[d]	178.6(4)	178.2(4)	177.8(4)	177.7(3)	178.1	1.348(5)	1.254(5)	1.309(5)	1.253(5)	1.344(5)	0.0555
1e	GP[e,f]	178.34	178.81	179.18	179.13	178.87	1.3355	1.2537	1.2960	1.2540	1.3350	0.0423
1e	DCM[e,g]	178.63	178.92	179.32	179.13	179.00	1.3361	1.2542	1.2967	1.2544	1.3357	0.0424
1f	GP[e,f]	177.46	178.00	177.68	177.07	177.55	1.3339	1.2540	1.2953	1.2535	1.3349	0.041[illegible]3
1f	DCM[e,g]	177.50	178.39	178.05	177.79	177.93	1.3346	1.2544	1.2960	1.2539	1.3356	0.0416

[a] See Figure 3 for atomic numbering. [b] Averaged bond angle of C1–C2–C3, C2–C3–C4, C3–C4–C5, and C4–C5–C6. [c] As calculated as the bond-length difference between C3–C4 and the average of C2–C3 and C4–C5. [d] X-ray crystallographic analysis. [e] Results from DFT calculations with the PBE0 density functional and the cc-pVTZ basis set. [f] Geometry optimization in the gas phase. [g] Geometry optimization in implicit dichloromethane solvent.

^{13}C NMR analysis. Experimentally, the ^{13}C NMR chemical shifts of tetraaryl[5]cumulenes have not been extensively studied,[47] but shifts in unstrained systems follow a characteristic pattern alternating upfield and downfield chemical shifts as observed for structurally related polyynes.[48,49] Using tetraphenyl[5]cumulene (**[5]Ph**) as a starting point (Table 3), the individual carbons can be assigned based on ^{13}C labelling of the terminal sp^2-hybridized carbons (C1/C6) of the cumulenic chain (see SI for details). Carbons C1/C6 resonate the farthest upfield (at 125 ppm), and the next carbon in the chain, sp-hybridized carbons C2/C5, resonate downfield at ca. 149 ppm. Finally, the central ^{13}C nuclei (C3/C4) are observed slightly downfield from C1/C6 at ca. 128 ppm. The ^{13}C NMR spectra for **1a–f** confirm that the molecules are, on average, symmetrical in solution (Figure 4). The individual resonances for carbons of the cumulenic core of **1c–e** have been assigned through C–H correlation experiments (see SI for details) and extrapolated to **1a**, **1b**, and **1f**. The ^{13}C NMR spectra for **1a–f** show resonances at values consistent with **[5]Ph**, with values C1/C6 of 124.1–124.5 ppm, C2/C5 of 149.4–149.9 ppm, and C3/C4 of 127.6–127.9 ppm. Overall, a slight

10.1002/chem.202200616

upfield shift for C1/C6 and a slight downfield shift for C2/C5 as a function of increasing strain are observed for resonances of the cumulene framework. The changes are quite small, however, particularly when compared to those reported for strained cyclic alkynes, including diynes[50] and tetraynes.[27]

To provide comparisons to experimentally measured ^{13}C shift values, resonances have been evaluated by DFT calculations using gas phase geometries (Table 3). Computed chemical shifts match the general trend of C1/C6 as the most upfield and C2/C5 as the most downfield signal, whereas the explicit values of the chemical shifts are shifted slightly lower in the cases of C1/C6 (~6 ppm) and C3/C4 (~5 ppm). Consistent with experimental observations, the computations predict a slight upfield shift for C1/C6 resonances as a function of ring strain, while a downfield shift is predicted for both C2/C5 and C3/C4.

Table 3. Experimental and calculated ^{13}C chemical shifts (ppm) for cumulenes **1a–f**.

cmpd	δ C1/C6		δ C2/C5		δ C3/C4	
	exp[a]	calc[b]	exp[a]	calc[b]	exp[a]	calc[b]
1a	124.1	118.5	149.8	149.1	127.7	123.0
1b	124.1	118.3	149.9	148.4	127.6	123.4
1c	124.2	118.6	149.6	148.6	127.7	122.7
1d	124.3	118.7	149.4	148.4	127.7	122.7
1e	124.4	118.7	149.5	148.3	127.7	122.7
1f	124.5	118.4	149.5	148.0	127.9	122.6
[5]Ph	124.7	119.1	149.4	147.4	127.3	121.7

[a] Experimentally measured in $CDCl_3$. [b] Calculated at the PBE0/cc-pVTZ level of theory in implicit $CDCl_3$ solvent from gas phase geometries.

10.1002/chem.202200616

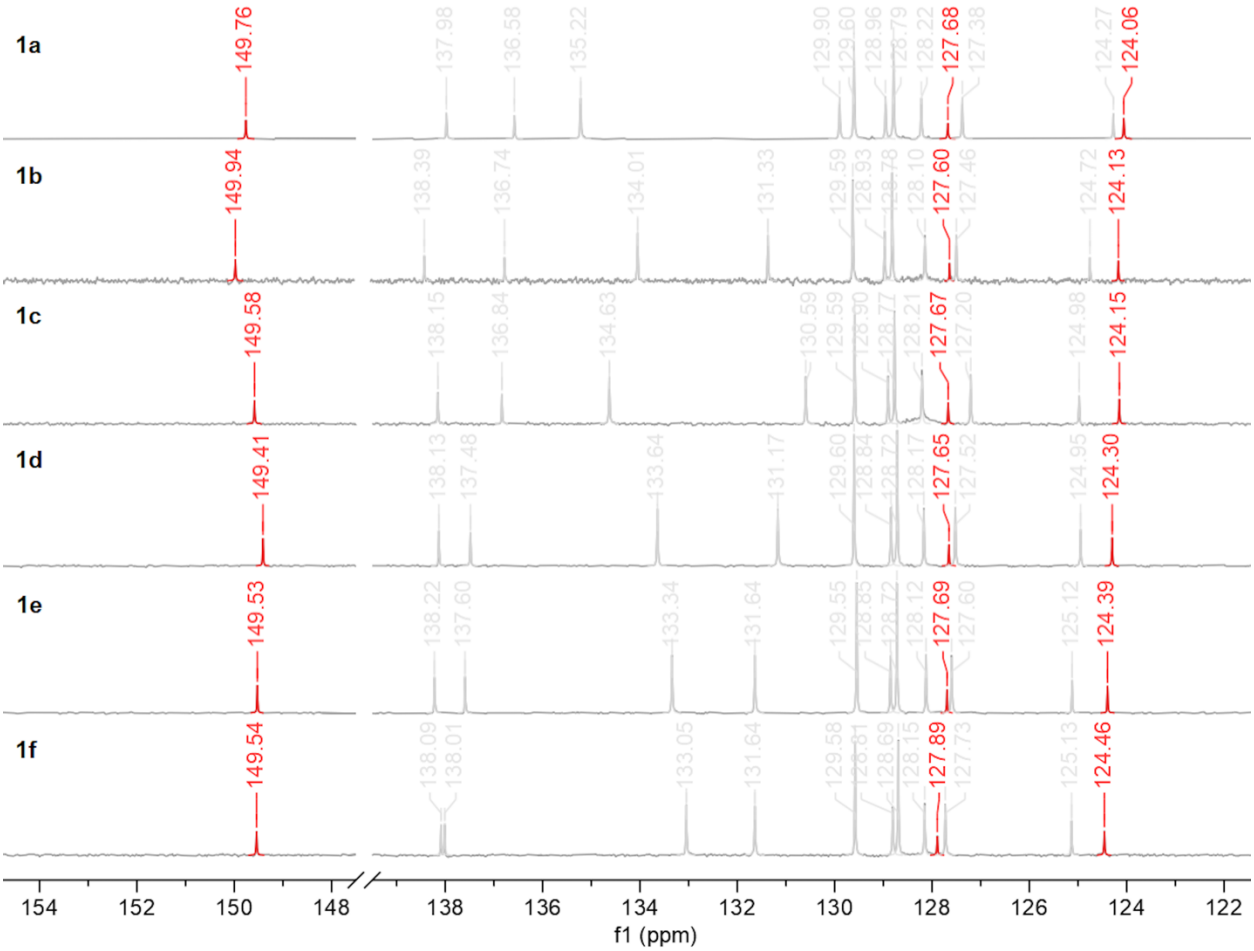

Figure 4. ^{13}C NMR (125 MHz) spectra of compounds **1a**–**f** measured in $CDCl_3$, cumulenic carbon signals highlighted in red, C2/C5, C3/C4, and C1/C6 (from left to right).

UV-vis spectroscopy. In general, acyclic [*n*]cumulenes possess two sets of conjugated, albeit orthogonal, π-orbital systems. One π-system is formally perpendicular to the molecular plane, including the cumulene framework and further conjugates to aryl end groups (Figure 5a, out-of-plane, OOP, orbitals shown in red). The second π-system lies in the molecular plane and is effectively limited to the four π-orbitals of the sp-carbons of the cumulene (Figure 5a, in-plane, IP, orbitals shown in blue).[51,52] The situation is somewhat more complicated for cyclic cumulenes,

10.1002/chem.202200616

in which the two π-systems are not formally orthogonal due to the constraints of the alkyl chain (see SI for details and orbital descriptions).

Experimentally, the UV-vis spectrum of each cumulene **1a–f** measured in dichloromethane shows four major absorptions (Figure 5b, Table 4). The lowest-energy electronic transition (λ_{max}) arises from the OOP π-system and gives rise to a major absorption peak near 500 nm (Figure 5b, Table 4). Calculations confirm these absorptions corresponds to the HOMO to LUMO transition (Figure 6a). A mild red shift is observed in this absorption as ring strain in increased, from 494 nm (**1f**) to 504 nm (**1a**).[53] The minimal dependence for the optical band gap versus strain of the cumulene framework has been previously predicted through calculations for carbyne,[54] and it is consistent with our calculations in which the HOMO and LUMO orbital energies do not change significantly for the compounds **1a–1f** (Figure 6b). In addition to the HOMO to LUMO band, two lower intensity absorption peaks are also observed for all compounds at ca. 440 nm (λ_3) and 370 nm (λ_2). These bands are assigned as the HOMO – 3 to LUMO and either the HOMO – 1 to LUMO (**1a** and **1d–f**) or the HOMO to LUMO + 1 (**1b–c**) transitions, respectively. Both λ_3 and λ_2 arise from transitions from the IP to OOP orbitals, which are no longer formally forbidden due to twisting of the molecular structure away from planarity, albeit oscillator strengths for these transitions are weak (see calculated values, Table S3). The strong λ_1 band is observed at ca. 280 nm and assigned by calculations as the HOMO to LUMO + 5 and HOMO to LUMO + 4 transitions. In the experimental spectra, this band is sometimes split into two closely spaced absorptions, and the computed spectra also report absorptions as a shoulder to the λ_1 peak (Table S3).

Thus, experimental results show a red shift in absorptions as a function of increasing ring strain moving from **1f** to **1a** for all four absorptions (λ_1, λ_2, λ_3, and λ_{max}), although the changes are

10.1002/chem.202200616

less than 0.16 eV in all cases. Trends in the calculated transition energies, on the other hand, are less pronounced (Table 4).

The lowest energy transition originating from the IP π-system is calculated to lie between 263–268 nm for **1a–1f**, and the predominant character is assigned to the HOMO – 3 to LUMO + 1 transition (Table 4). This computed transition is likely associated with the intense absorption at 250 nm in the experimental spectrum (Figure 5b). While at the limit of the accessible measurement range for solutions of **1a–1f**, both experiment and calculations suggest that this transition changes little as strain is increased.

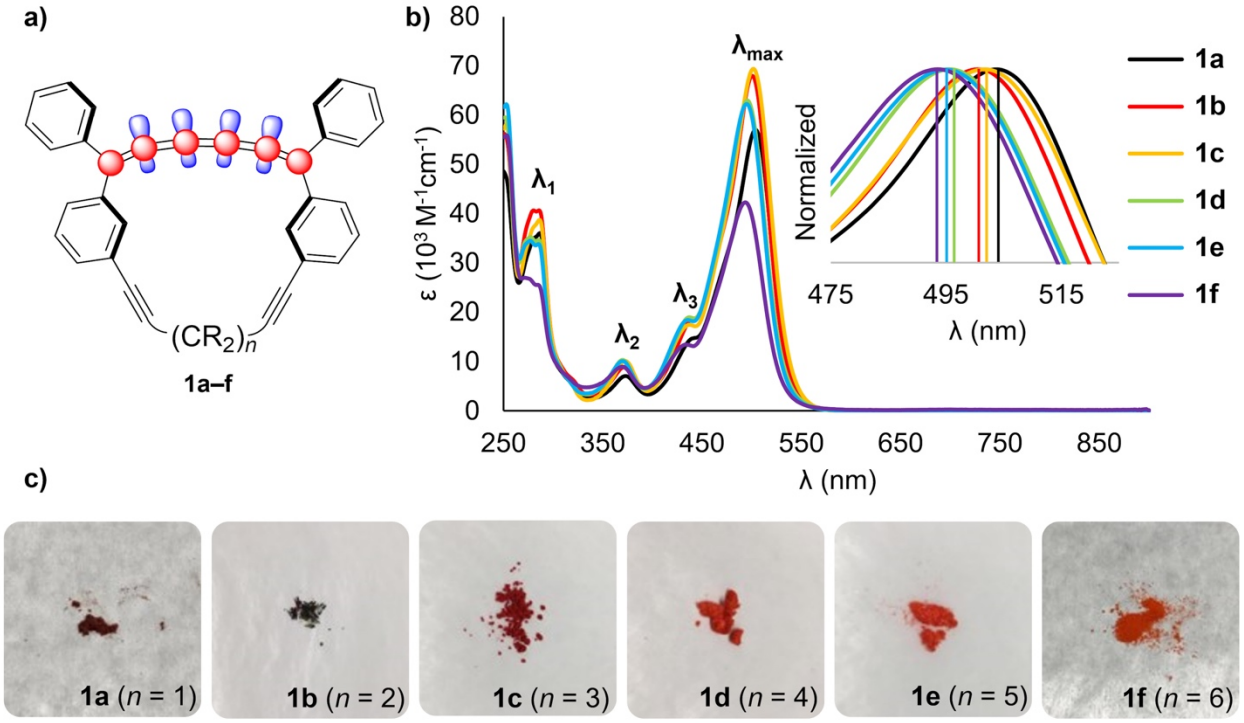

Figure 5. a) Schematic drawing of in- and out-of-plane π-orbital systems for **1a–f** (blue and red, respectively); b) UV-vis spectra of compounds **1a–f** measured in CH_2Cl_2, with expansion of the region 475–525 nm; and c) pictures of **1a–f** as solids.

10.1002/chem.202200616

It is interesting to note that the color of the compounds as solids becomes darker as ring strain increases indicating a different absorption behavior from solution (Figure 5c). On the basis of packing observed from single crystal analysis, however, there is no obvious explanation that accounts for the differing behavior in the solid state and solution.

Table 3. Selected UV-vis and Raman spectral data for compounds **1a**–**f**.

	UV-Vis						Raman[e]
cmpd	λ_{IP} (nm) calc[a,b]	λ_1 (nm) exp/calc[a]	λ_1 (nm) exp/calc[a]	λ_2 (nm) exp/calc[a]	λ_3 (nm) exp/calc[a,c]	λ_{max} (nm) exp/calc[a,d]	ν (cm^{-1}) exp/calc[f]
1a	268	282[g]/276[h]	286/281[i]	373/378[j]	443/448	504/504	1978.6/2167.5
1b	263	280/278[k]	286/281[i]	372/383[l]	440/432	501/521	1981.8/2172.5
1c	266	282[g]/277[k]	286/282[h]	372/367[l]	437/446	502/499	1979.8/2169.5
1d	266	277/279[k]	285/282[h]	370/372[j]	437/445	496/495	1982.1/2171.5
1e	266	277/279[i]	285/282[h]	370/376[j]	436/445	495/498	1983.4/2175.7
1f	266	272/278[k]	285/283[h]	369/377[j]	434/443	494/503	1981.8/2171.2

[a] Excitations computed at the PBE0/cc-pVTZ level of theory with TD-DFT in the gas phase. [b] HOMO – 3 to LUMO + 1. [c] HOMO – 3 to LUMO. [d] HOMO to LUMO. [e] Position of the Я line as determined by band fitting of the Raman spectra collected in chloroform solutions (see SI for details). [f] Computed at the PBE0/cc-pVTZ level of theory with implicit solvation in $CHCl_3$. [g] Shoulder absorption. [h] HOMO to LUMO + 5. [i] HOMO to LUMO + 4. [j] HOMO – 1 to LUMO. [k] HOMO to LUMO + 6. [l] HOMO to LUMO + 1.

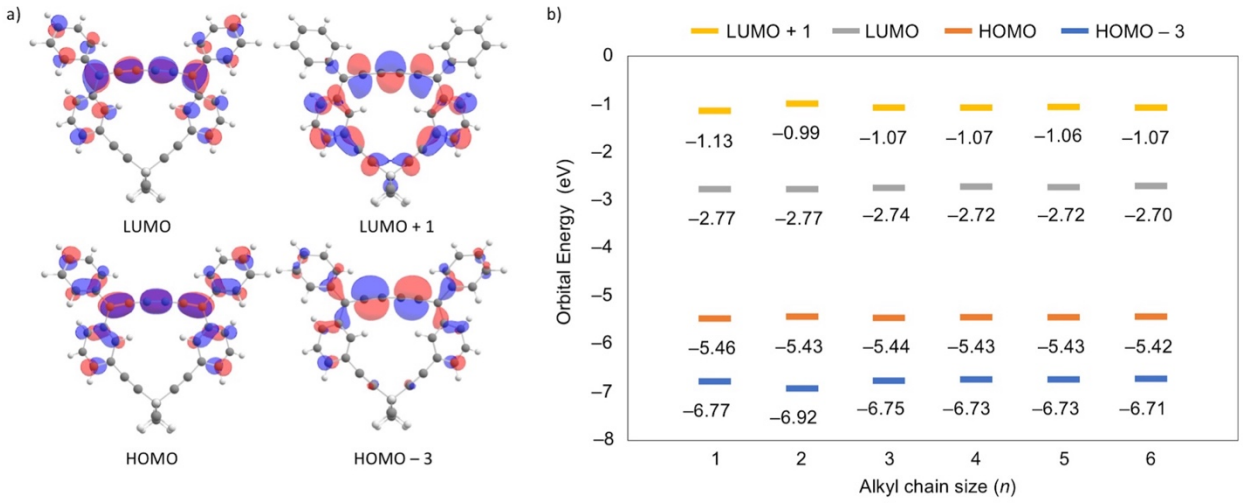

10.1002/chem.202200616

Figure 6. a) Orbitals involved in lowest energy transitions λ_{max} (HOMO → LUMO) and λ_{IP} (HOMO – 3 → LUMO + 1) for **1a** (computed at the PBE0/cc-pVTZ level of theory in the gas phase), and b) computed orbital energies as a function of ring size.

Raman analysis. Vibrational spectroscopy has been used to define trends as a function of ring strain for cyclic diynes[50] and tetraynes,[55] based on the distinctive Я line of the oligoyne chain (longitudinal CC stretching modes, also known in the literature as Effective Conjugation Coordinate, ECC, modes).[56] To date, reported studies of cumulenes are limited to linear tetraaryl[*n*]cumulenes and highlight important contributions from the pendent aryl rings.[57] The Raman spectra for cyclic [5]cumulenes **1b–f** have been measured in solutions of $CHCl_3$ (concentrations of 5–6 mM), and the position of the Я line is reported in Table 4 (spectra are provided in the SI). Unfortunately, the Я line of **1a** could not be reliably established due to the formation of dimer **6** during sample preparation and measurement. For this reason, the Я line of **1a** cannot be considered in the analysis reported below, which is based on small shifts of the Я line that could be easily affected by the onset of chemical reactions in the sample.

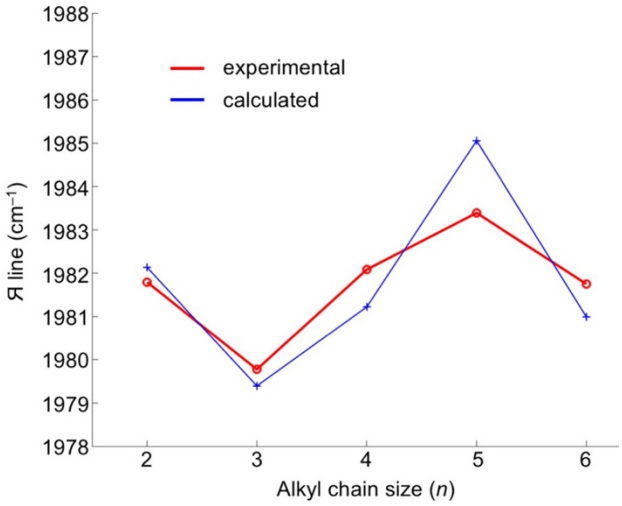

Figure 7. Trends in the position of the Я line as a function of alkyl chain size (*n*) in cyclic [*n*]cumulenes **1b–f**, based on experimental data ($CHCl_3$ solutions) compared with scaled results from DFT calculations (calculated at the PBE0/cc-pVTZ level of theory in implicit $CHCl_3$ solvent from gas phase geometries, see SI for details). The calculated frequencies of the Я lines have been scaled by 0.912.

In comparison to cyclic tetraynes that have been previously investigated (see Figure 1c),[55] the Я line of **1b–f** is surprisingly insensitive to increasing ring strain, and values for all derivatives are found in a narrow range of 1979–1983 cm^{-1} (Table 4). To understand this behavior, the Raman response of **1b–f** has been explored through a series of DFT calculations. The results from DFT calculations match the observed trend in the position of the Я line of the five cyclic cumulenes **1b–f** (Table 4 and Figure 7). DFT consistently overestimates the wavenumber of the Я line and a scaling factor 0.912 has been used to normalize the calculated values with those determined experimentally. The largest discrepancy between theory and experiment is found for the compound **1e**, whereas for the other cases the agreement is very good. Even though the variations of the peak positions from molecule to molecule are very minor (just a few cm^{-1}), the trend of the Я lines is fully supported by the DFT results. While the position of the Я line for cyclic tetraynes show a monotonic change as a function of the length (n) of the alkyl chain and increased strain,[55] data for the cyclic cumulenes **1b–f** are curved vs. n, which deserves further analysis. Two possible explanations for the behavior of the Я line of **1b–f** appear plausible. On the one hand, as discussed for oligoynes,[55] the bending of the sp-chain induced by the alkyl chains of different length may affect the position of the ECC mode. Since the average bond angle along the cumulene chain range increases monotonically from 175° to 179° in **1b–f**, dependent on the length of the alkyl chain (Table 2, BA_{avg}), the curved relationship in Figure 7 can be discarded.

On the other hand, the HOMO and LUMO orbitals of the cyclic cumulenes are delocalized along the cumulene chain and the aryl moieties (as shown in Figure 6a for **1a**). Indeed, previous studies of tetraaryl[n]cumulenes[57] show that the aryl groups are electronically coupled to the π-electrons of the cumulene chain. Thus, any change in the relative orientation of the aryl rings relative to the π-orbitals of the sp-chain should also affect the vibrational frequency of the ECC mode as probed by Raman spectroscopy. Therefore, analysis is directed to the four dihedral angles (φ) formed by the aryl groups and the cumulene chain, approximating the relative position of the 2p lobes of the cumulene and that of the aryl plane, as indicated in Figure 8. By construction, for a given aryl substituent, the angle φ is formed between the axis of the 2p lobes belonging to the cumulene and the axis orthogonal to the aryl plane. The cos(φ) dependence of π-conjugation in apolar systems has been outlined, based on the conformational torsion angle between two conjugated moieties.[58] Therefore, the average of the cosine of the four angles φ is used here as a simple collective variable (ξ) to describe the effect of the cumulene-aryl coupling:

10.1002/chem.202200616

$$\xi = \frac{1}{4}\sum_{i=1}^{4}\cos(\phi_i) \qquad \text{(eq 1)}$$

The relationship between the Я line and ξ is remarkable (Figure 8), clearly linking the observed experimental data for cumulenes **1b**–**f** and orientation of the aryl groups. This relationship is also supported and confirmed for two linear [5]cumulenes, namely [5]Ph[59] and [5]TrTol.[60] Thus, this Raman analysis provides convincing evidence that the effect on the position of the Я line from bending of the sp-chain is minor in comparison to the modulation caused by the conformation of the pendent aryl substituents for the cyclic cumulenes here considered (**1b**–**f**).

a)

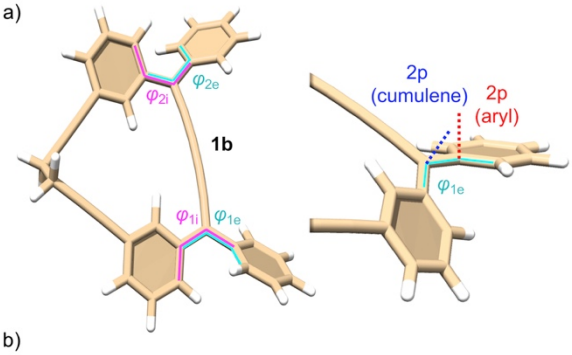

b)

cmpd	*n*	Я line (cm^{-1})	φ_{1i} (°)	φ_{1e} (°)	φ_{2i} (°)	φ_{2e} (°)	ξ (unitless)
1b	2	1981.8	–19	–41	–19	–41	0.85
1c	3	1979.8	–35	–31	25	36	0.85
1d	4	1982.1	–27	–36	38	29	0.84
1e	5	1983.4	36	30	–36	–30	0.84
1f	6	1981.8	–23	–41	40	27	0.83
[5]Ph	--	1981.4	–32	–32	–32	–32	0.84
[5]TrTol	--	1986.9	–26	–45	45	25	0.80

c)

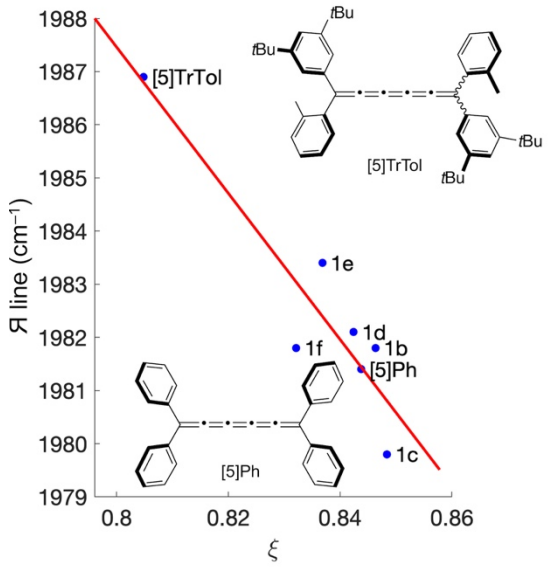

Figure 8. a) Representation of the molecular structure of **1b** describing the definition of the dihedral φ in relation to the angle formed from axes that approximate the 2p orbitals of the cumulene and of the aryl substituents. b) DFT-computed values of the individual dihedral angles φ that have been used to compute ξ for **1b–f** in comparison to linear [5]cumulenes [5]Ph and [5]TrTol. c) Linear regression ($\mathit{Я}$ = 2097.45 – 137.48 ξ; R^2 = 0.85) describing the position of the Я line as a function of the average cosine (ξ) of the dihedral angles (φ) according to eq 1.

In conclusion, a series of cyclic tetraaryl[5]cumulenes has been synthesized to study the effects of ring strain on physical and spectroscopic properties. X-ray crystallography shows cumulenic bond angles in the solid state are reduced to as little as 172.3° in the macrocycle tethered with the shortest alkyl chain, **1a**. Structures optimized by DFT calculations give bond angles comparable to those determined crystallographically. Reactivity of the cyclic products increases with strain, culminating in **1a**, which readily undergoes dimerization in solution at ambient temperatures to give the radialene product **6**. Spectroscopic analyses and DFT calculations confirm minor trends in the ^{13}C NMR and UV-vis spectra as a function of increasing strain, while no discernible trends are found in bond length alternation through X-ray crystallographic analysis. The Raman shifts of the Я line as a function of the increasing strain show minor variations, but no consistent trend as a function of the length of the alkyl chain. Close inspection, however, clearly links the position of the Я line to electronic coupling between the cumulene and aryl moieties. More specifically, the position of the Я line relates linearly to conformations of the pendent aryl groups, determined as a function of the average cosine of the angle formed by the 2p orbitals of the cumulene and the aryl groups. Within the range of strained [5]cumulenes that are synthetically accessible through the current study and analyzed computationally, it is demonstrated that strain has only a minor impact on the observably physical and spectroscopic properties.

10.1002/chem.202200616

Acknowledgements

RRT and MK are grateful for funding of this work from the Natural Sciences and Engineering Research Council of Canada (NSERC). MK and MSO appreciate the support for calculations provided by Compute Canada (www.computecanada.ca). RRT acknowledges support from the Canada Foundation for Innovation (CFI) and the Deutsche Forschungsgemeinschaft (SFB 953, "Synthetic Carbon Allotropes"). MT and AL are grateful for funding of this work from the European Research Council (ERC) under the European Union's Horizon 2020 research and innovation program ERC-Consolidator Grant (ERC CoG 2016 EspLORE grant agreement no. 724610, website: www.esplore.polimi.it).

References

[1] A. L. Sadowy, R. R. Tykwinski, in *Modern Supramolecular Chemistry: Strategies for Macrocycle Synthesis* (Eds.: F. Diederich, P. J. Stang, R. R. Tykwinski), Wiley-VCH, **2008**, pp. 185–231.

[2] C. E. Colwell, T. W. Price, T. Stauch, R. Jasti, *Chem. Sci.* **2020**, *11*, 3923–3930.

[3] F. Sondheimer, *Acc. Chem. Res.* **1972**, *5*, 81–91.

[4] E. L. Spitler, C. A. Johnson II, M. M. Haley, *Chem. Rev.* **2006**, *106*, 5344–5386.

[5] K. Cocq, C. Lepetit, V. Maraval, R. Chauvin, *Chem. Soc. Rev.* **2015**, *44*, 6535–6559.

[6] T. Kawase, H. Kurata, *Chem. Rev.* **2006**, *106*, 5250–5273.

[7] M. K. Smith, O. Š. Miljanić, *Org. Biomol. Chem.* **2015**, *13*, 7841–7845.

[8] M. Hermann, D. Wassy, B. Esser, *Angew. Chem. Int. Ed.* **2021**, *60,* 15743–15766.

[9] K. Tahara, Y. Tobe, *Chem. Rev.* **2006**, *106*, 5274–5290.

[10] M. Iyoda, J. Yamakawa, M. J. Rahman, *Angew. Chem. Int. Ed.* **2011**, *50*, 10522–10553.

[11] Y. Liang, M. Tang, Z. Liu, *Chem. Lett.* **2020**, *49*, 1329–1336.

[12] M. A. Majewski, M. Stępień, *Angew. Chem. Int. Ed.* **2019**, *58*, 86–116.

[13] S. Liu, Y. Lei, X. Qi, Y. Lan, *J. Phys. Chem. A* **2014**, *118*, 2638–2645.

[14] Y. Xu, M. von Delius, *Angew. Chem. Int. Ed.* **2020**, *59*, 559–573.

[15] K. Miki, K. Ohe, *Chem. Eur. J.* **2020**, *26*, 2529–2575.

[16] E. J. Leonhardt, R. Jasti, *Nat. Rev. Chem.* **2019**, *3*, 672–686.

[17] F. Liebman, A. Greenberg, *Chem. Rev.* **1976**, *76*, 311–365.

[18] H. L. Anderson, C. W. Patrick, L. M. Scriven, S. L. Woltering, *Bull. Chem. Soc. Jpn.* **2021**, *94*, 798–811.

[19] Y. Tobe, T. Wakabayashi, in *Polyynes: Synthesis, Properties, and Applications*; F. Cataldo, Ed.; CRC Press/Taylor & Francis Boca Raton, **2006**, 99–125.

[20] C. S. Casari, M. Tommasini, R. R. Tykwinski, A. Milani, *Nanoscale* **2016**, *8*, 4414–4435.

[21] Y. Gao, Y. Hou, F. Gordillo Gámez, M. J. Ferguson, J. Casado, R. R. Tykwinski, *Nat. Chem.* **2020**, *12*, 1143–1149.

[22] A. E. Boguslavskiy, H. Ding, J. P. Maier, *J. Chem. Phys.* **2005**, *123*, 034305.

[23] F. Diederich, Y. Rubin, O. L. Chapman, N. S. Goroff, *Helv. Chim. Acta* **1994**, *77*, 1441–1457.

[24] K. Kaiser, L. M. Scriven, F. Schulz, P. Gawel, L. Gross, H. L. Anderson, *Science* **2019**, *365*, 1299–1301.

[25] L. M. Scriven, K. Kaiser, F. Schulz, A. J. Sterling, S. L. Woltering, P. Gawel, K. E. Christensen, H. L. Anderson, L. Gross, *J. Am. Chem. Soc.* **2020**, *142*, 12921–12924.

[26] A. La Torre, A. Botello-Mendez, W. Baaziz, J. C. Charlier, F. Banhart, *Nat. Commun.* **2015**, *6*, 6636–6642.

[27] A. Spantulescu, T. Luu, Y. Zhao, R. McDonald, R. R. Tykwinski, *Org. Lett.* **2008**, *10*, 609–612.

[28] R. P. Johnson, *Chem. Rev.* **1989**, *89*, 1111–1124.

[29] S. Hernandez, M. M. Kirchhoff, S. G. Swartz, R. P. Johnson, *Tetrahedron Lett.* **1996**, *37*, 4907–4910.

[30] R. O. Angus, R. P. Johnson, *J. Org. Chem.* **1984**, *49*, 2880–2883.

[31] For prior examples of unstrained, cyclic tetraalkyl[5]cumulenes, see T. Negi, T. Kaneda, H. Mizuno, T. Toyoda, Y. Sakata, S. Misumi, *Bull. Chem. Soc. Jpn.* **1974**, *47*, 2398–2405.

[32] J. A. Januszewski, R. R. Tykwinski, *Chem. Soc. Rev.* **2014**, *43*, 3184–3203.

[33] D. Wendinger, R. R. Tykwinski, *Acc. Chem. Res.* **2017**, *50*, 1468–1479.

[34] L. Balas, T. Durand, S. Saha, I. Johnson, S. Mukhopadhyay, *J. Med. Chem.* **2009**, *52*, 1005–1017.

[35] J. L. Marshall, D. Lehnherr, B.D. Lindner, *ChemPlusChem* **2017**, *82*, 967–1001.

[36] M. Gholami, R. R. Tykwinski, *Chem. Rev*. **2006**, *106*, 4997–5027.

[37] H. D. Hartzler, *J. Am. Chem. Soc*. **1971**, *93*, 4527–4531.

[38] N. Islam, T. Ooi, T. Iwasawa, M. Nishiuchi and Y. Kawamura, *Chem. Commun*. **2009**, 574–576.

[39] D. Wendinger, J. A. Januszewski, F. Hampel, R. R. Tykwinski, *Chem. Commun.* **2015**, *51*, 14877–14880.

[40] Y. Kuwatani, G. Yamamoto, M. Oda, M. Iyoda, *Bull. Chem. Soc. Jpn.* **2005**, *78*, 2188–2208.

[41] K. J. Daoust, S. M. Hernandez, K. M. Konrad, I. D. Mackie, J. Winstanley, Jr., R. P. Johnson, *J. Org. Chem.* **2006**, *71*, 5708–5714

[42] Deposition Number(s) <url href="https://www.ccdc.cam.ac.uk/services/structures?id=doi:10.1002/chem.202200616"> 2089313 (for **1a**), 2089314 (for **1b**), 2089315 (for **1c**), 2089892 (for **1d**), 2089893 (for **1e**)</url> contain(s) the supplementary crystallographic data for this paper. These data are provided free of charge by the joint Cambridge Crystallographic Data Centre and

Fachinformationszentrum Karlsruhe <url href=" http://www.ccdc.cam.ac.uk/structures ">Access Structures service</url>

[43] J. A. Januszewski, D. Wendinger, C. D. Methfessel, F. Hampel, R. R. Tykwinski, *Angew. Chem. Int. Ed.* **2013**, *52*, 1817–1821.

[44] C. Adamo, V. Barone, *J Chem. Phys*. **1999**, *110*, 6158–6169.

[45] T. H. Dunning Jr., *J. Chem. Phys*. **1989**, *90*, 1007–1023.

[46] S. E. Wheeler, *WIREs Comput. Mol*. Sci. **2012**, *2*, 204–220.

[47] For theoretical predictions, see: K. B. Wiberg, J. D. Hammer, K. W. Zilm, J. R. Cheeseman, *J. Org. Chem.* **1999**, *64*, 6394–6400.

[48] R. R. Tykwinski, T. Luu, *Synthesis* **2012**, *44*, 1915–1922.

[49] A. Ehnbom, M. B. Hall, J. A. Gladysz, *Org. Lett.* **2019**, *21*, 753–757.

[50] S. Eisler, R. McDonald, G.R. Loppnow, R.R. Tykwinski, *J. Am. Chem. Soc*. **2000**, *122*, 6917–6928.

[51] This analysis is adapted from linear [*n*]cumulenes (see reference 52) and is, of course, an over simplification, but it allows the formal designation of the two π-systems that dominate the electronic characteristics of these molecules.

[52] M. Franz, J.A. Januszewski, D. Wendinger, C. Neiss, L.D. Movsisyan, F. Hampel, H.L. Anderson, A. Görling, R.R. Tykwinski, *Angew. Chem*. *Int. Ed.* **2015**, *54*, 6645–6649.

[53] The electronic absorption spectra of unstrained, cyclic tetraalkyl[5]cumulenes has been described, see reference 31.

[54] Y. H. Hu, *J. Phys. Chem. C* **2011**, *115*, 1843–1850.

[55] A. Lucotti, M. Tommasini, W.A. Chalifoux, D. Fazzi, G. Zerbi, R.R. Tykwinski, *J. Raman Spectr.* **2012**, *43*, 95–101.

[56] C. Castiglioni, M. Tommasini, G. Zerbi, *Philos. Trans. R. Soc. A* **2004**, *362*, 2425−2459.

[57] M. Tommasini, A. Milani, D. Fazzi, A. Lucotti, C. Castiglioni, J.A. Januszewski, D. Wendinger, R. R. Tykwinski, *J. Phys. Chem. C* **2014**, *118*, 26415–26425.

[58] A. Troisi, A. Shaw, *J. Phys. Chem. Lett.* **2016**, *7*, 4689–4694.

[59] See Supporting Information for synthetic details.

[60] M. U. Bühringer, K. Padberg, M. D. Phleps, H. Maid, C. Placht, C. Neiss, M. J. Ferguson, A. Görling, R. R. Tykwinski, *Angew. Chem. Int. Ed.* **2018***, 57*, 8321–8325.

10.1002/chem.202200616

Keywords: cumulenes; macrocycles; Raman spectroscopy; ring strain; X-ray crystallography

Entry for the Table of Contents

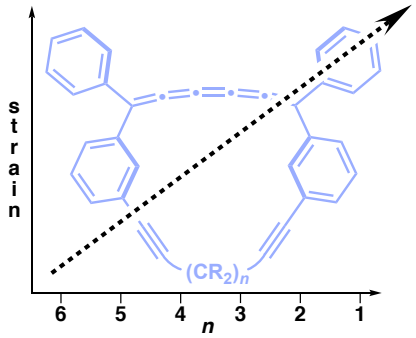

A series of cyclic tetraaryl[5]cumulenes is synthesized. In the smallest of the cycles, bond angles of the cumulene are distorted to as little as 172–174° based on crystallographic and computational analyses. Spectroscopic and physical properties as a function of ring size show small, but consistent, trends as ring strain increases.

Twitter usernames: @TykwinskiGroup; @meaganoakley